PCCP

Generation and structural characterization of Ge carbides GeC_n (*n = 4, 5, 6*) and GeC_5 by laser ablation, broadband rotational spectroscopy, and quantum chemistry

Journal:	*Physical Chemistry Chemical Physics*
Manuscript ID	CP-ART-06-2019-003607.R1
Article Type:	Paper
Date Submitted by the Author:	08-Aug-2019
Complete List of Authors:	Lee, Kelvin; Harvard-Smithsonian Center for Astrophysics, Thorwirth, Sven; Universität zu Köln, I. Physikalisches Institut Martin-Drumel, Marie-Aline; Harvard-Smithsonian Center for Astrophysics McCarthy, Michael C.; Harvard-Smithsonian Center for Astrophysics, AMP Division

Journal Name

ARTICLE TYPE

Cite this: DOI: 10.1039/xxxxxxxxxx

Generation and structural characterization of Ge carbides GeC_n ($n = 4, 5, 6$) by laser ablation, broadband rotational spectroscopy, and quantum chemistry†

Kin Long Kelvin Lee,*[a] Sven Thorwirth,[b‡], Marie-Aline Martin-Drumel[c‡] and Michael C. McCarthy[a]

Received Date
Accepted Date

DOI: 10.1039/xxxxxxxxxx

www.rsc.org/journalname

Following the recent discovery of T-shaped GeC_2, rotational spectra of three larger Ge carbides, linear GeC_4, GeC_5, and GeC_6 have been observed using chirped pulse and cavity Fourier transform microwave spectroscopy and a laser ablation molecule source, guided by new high-level quantum chemical calculations of their molecular structure. Like their isovalent Si-bearing counterparts, Ge carbides with an even number of carbon atoms beyond GeC_2 are predicted to possess $^1\Sigma$ ground electronic states, while odd-numbered carbon chains are generally $^3\Sigma$; all are predicted to be highly polar. For the three new molecules detected in this work, rotational lines of four of the five naturally occurring Ge isotopic variants have been observed between 6 and 22 GHz. Combining these measurements with *ab initio* force fields, the Ge−C bond lengths have been determined to high precision: the derived values of 1.776 Å for GeC_4, 1.818 Å for GeC_5, and 1.782 Å for GeC_6 indicate a double bond between these two atoms. Somewhat surprisingly, the spectrum of GeC_5 very closely resembles that of a $^1\Sigma$ molecule, implying a spin-spin coupling constant λ in excess of 770 GHz for this radical, a likely consequence of the large spin-orbit constant of atomic Ge ($\sim$1000 cm^{-1}). A systematic comparison between the production of SiC_n and GeC_n chains by laser ablation has also been been undertaken. The present work suggests that other large metal-bearing molecules may be amenable to detection by similar means.

1 Introduction

Small carbon clusters have been extensively studied by experiment and theory, and found almost exclusively to possess either linear, or highly symmetrical ring structures[1–4]. Substitution of one or more of these carbon atoms with the isovalent group 14 element silicon or germanium has profound consequences to molecular structure and polarity, which in turn often imparts these species with strong rotational spectra, a property that has enabled a number of small silicon carbides to be detected in circumstellar shells around certain evolved carbon stars[5]. Tricarbon and tetracarbon, for example, are only known experimentally to possess linear structures[1], but SiC_2,[6] Si_2C,[7], and Si_3[8] have bent or T-shaped geometries. For SiC_3, both linear and rhombic-shaped isomers are known,[9–12]. For still larger SiC_n clusters ($n = 4 - 8$), linear chains have been detected at high spectral resolution.[12]

In contrast, much less is known about the structure and bonding properties of the analogous Ge-bearing species. The interest in these species is to understand the underlying electronic structure of group 14 elements, and the nature of their chemical bonding. Until recently, only two Ge-species have been observed at high spectral resolution: germanium carbide (GeC) by low-temperature electronic emission[13], and one symmetric chain, GeC_3Ge, using infrared free-jet spectroscopy and a laser

[a] Center for Astrophysics | Harvard-Smithsonian, 60 Garden Street, Cambridge, Massachusetts 02138, USA; E-mail: kinlee@cfa.harvard.edu
[b] I. Physikalisches Institut, Universität zu Köln, Zülpicher Straße 77, 50937 Köln, Germany
[c] Institut des Sciences Moléculaires d'Orsay (ISMO), CNRS, Univ. Paris-Sud, Université Paris-Saclay, F-91405 Orsay, France

† Electronic Supplementary Information (ESI) available: [Includes tables of measured rotational lines and best-fit spectroscopic constants].

ablation source[14]. At lower spectral resolution, Graham and coworkers used Fourier transform infrared matrix isolation to measure the vibrational spectra of a number of Ge_nC_m clusters, including GeC_3Ge,[15] GeC_5Ge,[16] and three odd-numbered chains GeC_3[17], GeC_7, and GeC_9.[18]

Using chirped-pulsed (CP) and cavity Fourier-transform (FT) microwave spectroscopies[19], the rotational spectrum of GeC_2, the isovalent analog to C_3 and SiC_2, was reported by several of us recently. The species is produced so abundantly by laser ablation of a Ge:C rod that rotational lines of its ^{13}C isotopic species were observed in natural abundance in the chirped spectrum, despite the low fractional abundance of this isotope (1.1% natural abundance). This work, the first pure rotational investigation of a Ge-carbide cluster, enabled an unambiguous structure determination of the compound. Indeed, in contrast to prior quantum-chemical calculations[20–24] predicting an L-shaped structure as the global minimum on the potential energy surface, this carbide is found to be T-shaped instead. The structural controversy that surrounded GeC_2, much like early work on SiC_2[25], illustrates the importance of developing accurate theoretical descriptions of bonding that involve group 14 elements; the relevance of Si- and Ge-doped materials in semiconductor technology and nano/microelectronics[26–28], and the plethora of possible structures that are predicted even for small clusters, is another motivation to pursue accurate descriptions of their electronic structure.[29–34] For these reasons, there is great practical utility in studies of other small Ge carbides to benchmark theoretical methods so that chemical models with greater predictive power can be developed.

In this paper, we report the detection and characterization of three larger Ge-carbides, linear forms of GeC_4, GeC_5, and GeC_6 (Fig. 1). Guided by new coupled-cluster calculations of their structure, evidence was found for GeC_4 and GeC_5 chains in the broadband CP spectrum that initially enabled GeC_2 detection.[19] Subsequent measurements using cavity FT spectroscopy enabled both to extend the observations to higher frequency, and, based on high-level quantum-chemical calculations and empirical scaling factors, to specifically target and detect GeC_6. Precise rotational constants were determined for the most abundant Ge isotopic species without hyperfine interactions (^{74}Ge , ^{72}Ge, ^{70}Ge, ^{76}Ge), from which the Ge−C bond length has been derived to high accuracy in all three chains. In agreement with theoretical predictions and analogy to the pure carbon and silicon-carbon chains, clusters with an odd number of atoms (GeC_4 and GeC_6) are described by a closed-shell electronic configuration, while odd-numbered GeC_5 is an open-shell (triplet multiplicity) species, although its spectrum is otherwise indistinguishable from that of a $^1\Sigma$ molecule owing to a very large spin-spin constant λ. Finally, we draw parallels in the growth and relative abundance of germanium-carbon chains by comparison with analogous SiC_n experiments.

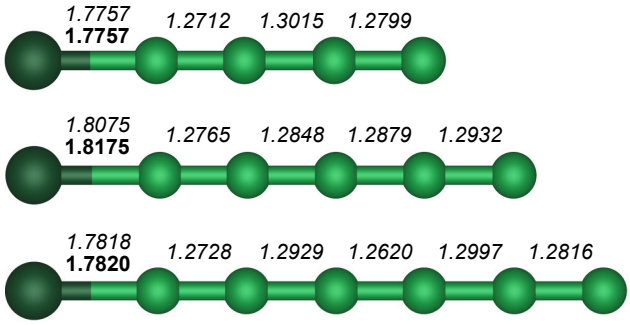

Fig. 1 Optimized structures of the GeC_n linear chains reported in this work. Geometries are adapted from CCSD(T)/cc-pwCVQZ calculations (italics). Empirical Ge−C bond lengths are given in bold face. See the Discussion section for details on the experimental structural determination.

2 Experimental Methods

Chirped-pulse Fourier-transform microwave (CP-FTMW) spectroscopy[35] followed by its cavity variant[36] were used to detect and analyze products formed in the laser ablation of a Ge:C rod. The combined approach of CP- and cavity FT spectroscopy has recently been used with good success to detect entirely new molecules,[37] such as $HC_4C(O)H$,[38] GeC_2,[19] and new vibrationally excited states of highly abundant species, such as C_2S and C_3S.[39] A real strength of this approach is that it exploits the advantages of both spectroscopies, in which the CP spectrum is used as a survey tool to detect "bright" resolution elements over a very wide frequency range, and cavity spectroscopy can then be efficiently used to rapidly analyze and characterize these smaller number of spectral features, owing to its higher instantaneous sensitivity and spectral resolution.

The laser ablation and microwave setups used for this experiment have been described in the previous publication on GeC_2[19] and are essential identical in design to that used previously to detect rotational lines of TiO_2.[40] In the present study, a 0.25 in diameter rod was formed by pressing a mixture of Ge and graphite powders (in the molar ratio 1:2) and a small amount of epoxy binder in a metal mold, and by applying two tons of pressure for 15 min. After curing for approximately 24 h, the rod was ablated using the second harmonic output of an Nd:YAG laser, corresponding to an unfocused pulse energy of 20 mJ/pulse. The 532 nm light was then focused onto the GeC rod with a 75 cm focal length lens; the energy density of the focused beam was found to optimize the production of SiC_2 using a rod of similar stoichiometry in preliminary experiments. The laser ablation pulse is synchronized with a pulsed nozzle so that the plume of ablated matter is entrained in an inert gas (Ne) and then expands adiabatically into a large vacuum chamber where both the CP and cavity spectrometers are co-located, but aligned along perpendicular axes. As is almost universally done in laser ablation

experiments of this kind, the rod was continuously rotated and translated so that each laser pulse ablates a new spot on the rod. The repetition rate of the laser and pulsed valve were 5 Hz.

2.1 Chirped-Pulse Measurements

The broadband spectrum of the laser ablation products from a Ge:C rod was recorded between 7 and 18 GHz by mixing a 4 μs chirp between 1 and 11.5 GHz with a phase-stable 19 GHz local oscillator. After amplifying the lower sideband (18–7 GHz), the chirp was sent to a 200 W traveling wave tube (TWT) for further amplification before it was broadcast between two matched horns, through which the gas pulse passes. The free induction decay (FID) was detected with a low-noise amplifier, but both a PIN diode and high isolation microwave switch are inserted just after the receive horn to protect this amplifier during the excitation pulse.

To improve the signal-to-noise ratio (SNR), each gas pulse was probed by 10 microwave chirps, each separated by 20 μs, where the FIDs associated with each are co-averaged on a fast digital oscilloscope (20 GHz) prior to transfer to a Linux workstation for real-time processing and analysis. At a sampling rate of 50 GSa/s, each FID consists of 750,000 points, yielding an instrumental resolution of 100 kHz. Because the phase stability is generally quite good, deep averages of at least several 100,000 gas pulses are feasible, although experimental factors such as changes in the nozzle tension and laser alignment often limit the effectiveness of very long integrations (i.e., >24 h). In total, the spectrum was accumulated for 17 h, corresponding to ~300,000 gas pulses at a repetition rate of 5 Hz. Subsequently, the intensity and frequency of all features in a specified bandwidth and with a specified SNR can be generated and monitored in real-time by using an automated peak finding algorithm. Upon the completion of the chirped experiment, instrumental artifacts and common contaminants are removed, and the resulting line list can be trivially converted to a batch file that can been be automatically executed with the cavity spectrometer software.[37] Known species are also systematically removed: for example, transitions of GeC_2 which were already assigned by Zingsheim *et al.*[19]

2.2 Cavity Measurements

Upon completion of the CP experiment, follow-up cavity measurements were immediately performed. This changeover is rapid (i.e., <3 min) because both spectrometers share much of the same equipment, including nozzle source, gas-flow system, timing circuitry, etc., and the only physical change required is to manually pullback a highly absorbent curtain that is placed in front of one of the cavity mirrors to spoil the cavity Q during CP operation. The cavity instrument used in the present investigation has been described in detail elsewhere,[41,42] but it operates between 5 and 26 GHz, so in addition to analysis and characterization, it can be used to extend the range of measurement, often to higher frequency.

The operation of the cavity spectrometer is similar to the CP instrument in that a short (1 μs) pulse of microwave radiation coherently excites molecules as they pass through the center of a high-Q ($10^4 - 10^5$) Fabry-Perot cavity. If a molecule possesses a rotational transition within the narrow frequency range of the pulse (~1 MHz), the FID is detected with a sensitive microwave receiver and the corresponding Fourier transform (performed on the computer) contains the frequency-domain spectrum. Owing to the high finesse of the cavity, its sensitivity per unit MHz is roughly 40 times greater than that of the CP spectrometer.[35] In addition, the linewidths of cavity-recorded transitions, normally determined by the time-of-flight through the active volume,[43] are typically at least 10 times sharper (2–4 kHz FWHM) than those in a CP spectrum, a feature which often allows closely-spaced hyperfine structure to be resolved.

3 Computational Methods

Quantum-chemical calculations of GeC_4, GeC_5, and GeC_6 were performed using coupled-cluster with single, double, and perturbative triple excitations [CCSD(T)][44] using the CFOUR suite of programs[45,46] in combination with Dunning's hierarchies of correlation-consistent polarized valence[47,48] and polarized core-valence basis sets.[49–52] Structure calculations were performed using the cc-pVXZ (X =D, T, Q) basis sets in the frozen core (fc) approximation, and with basis sets as large as cc-pwCVQZ when considering all-electrons (ae) in the CCSD(T) treatment. Harmonic, cubic, and semi-quartic force fields were calculated using the cc-pVXZ (X =D, T) bases in the fc approximation and analytic second-derivatives procedures[53] together with numerical differentiation for the third and fourth derivatives.[54,55] Due to the large computational expense associated with these calculations, the cc-pVTZ basis was only used for the smallest (GeC_4) species as a point of comparison. For the chains with an even number of carbon atoms, a closed-shell Hartree-Fock (HF) reference function was used, whereas an unrestricted HF (UHF) reference was used for GeC_5, which has a triplet ground state. For the latter, using the cc-pwCVQZ basis set, appreciable spin contamination is observed at the UHF level ($<S^2>$=2.40 translating into an approximate spin multiplicity of some 3.25) whereas at the unrestricted CCSD (UCCSD) level this is almost entirely resolved (projected $<S^2>$=2.11 and approximate spin multiplicity of 3.07).

4 Results

As illustrated in Fig 2, the most prominent features in the 7-18 GHz spectrum are the fundamental a-type rotational lines of T-shaped GeC_2 near 15.3 GHz, owing to the large number of germanium isotopes with significant fractional abundance (21%

^{70}Ge, 28% ^{72}Ge, 8% ^{73}Ge, 36% ^{74}Ge, and 8% ^{76}Ge). Beyond these features, nearly 100 other spectral features were identified with a SNR of three or greater. Nearly one half of these were assigned to known molecules including GeS, three cyanopolyyne chains HC_3N, HC_5N, and HC_7N, and two methyl acetylene chains CH_3CCH and CH_3C_4H using SPECDATA, a recently developed in-house database query system that rapidly assigns transitions of known species in an experimental spectrum.[56] The remaining features were subject to further scrutiny by cavity spectroscopy, and of these, roughly ten were either not observed within a few minutes of integration, not laser dependent, or exhibit narrow line (hyperfine) structure that is not consistent with the elemental composition of the pressed powder rod, suggesting that they likely arise from the binder, one of its by-products, or some other contaminant. However, approximately 20 lines, most of which lying between 7 and 10 GHz, were observed only when the laser was present and were structureless, suggesting the carrier or carriers must be Ge-bearing molecules, C-bearing, or both. Tables of observed frequencies and molecular parameters can be found in the Electronic Supplementary Information.

4.1 GeC_4

Guided by the quantum-chemical calculations in Sec. 3 (Table 1), a total of six lines of either $^{70}GeC_4$, $^{72}GeC_4$ or $^{74}GeC_4$ were assigned among the unidentified features, and closer inspection of the CP spectrum (Fig. 2) reveals additional features, albeit at lower SNR, at the expected frequencies of the less abundant $^{73}GeC_4$ species, or at either higher or lower predicted frequencies for the two most abundant species. Ultimately, at least five rotational transitions between 6 and 22 GHz were measured with the cavity spectrometer for all but $^{73}GeC_4$ (Table S1); owing to the larger rotational partition function due to hyperfine structure from the $I = 9/2$ nuclear spin of ^{73}Ge, no evidence was found for $^{73}GeC_4$ at the present SNR.

The observed lines were trivially analyzed using a standard Hamiltonian for a linear molecule. The best-fit rotational constants are summarized in Table 1 along with those predicted at the CCSD(T)/cc-pwCVQZ level of theory. The agreement between the sets of rotational constants is exceptional; the calculated values reproduce the measurements within $\sim$0.1% even with the lower quality force field (fc-CCSD(T)/cc-pVDZ).

4.2 GeC_5

Following discovery of GeC_4 in the CP spectrum in Fig. 2, attempts were made to identify lines of linear structures of GeC_3, GeC_5, and GeC_6. As illustrated in the plots at the bottom of this Figure, several harmonic series of lines near in frequency to those predicted for isotopic GeC_5 were readily identified; six of these were among the 20 or so lines that were previously found to be laser-dependent unidentified features in the cavity categorization tests. Because the lines are separated in frequency by ratios of integers, additional features were soon found with the cavity spectrometer. Table S3 provides a summary of the measurements, which range from $N = 6$ to 17, for $^{70}GeC_5$, $^{72}GeC_5$, and $^{74}GeC_5$.

Because the spectrum of GeC_5 is otherwise indistinguishable from that of $^1\Sigma$ molecule, magnetic tests were performed to establish that its lines are indeed sensitive to the presence of a weak magnetic field, as required for a radical with a $^3\Sigma$ ground state. As shown in Fig. 3, the intensity of the $7_6 \rightarrow 6_5$ line (and others) are significantly diminished when a permanent magnet is brought near the supersonic expansion. Although weak, the resulting line profiles are similar to those of radicals that have partially-resolved Zeeman structure (with $\Delta M_J = \pm 1$ transitions).

Like isovalent SiC_5, GeC_5 is predicted to possess a $^3\Sigma$ ground state. Thus, by analogy to other species with triplet multiplicity such as C_6S and C_8S,[57] lines from the F_2 ($J = N$) and F_3 ($J = N + 1$) spin components are expected to lie significantly higher in energy relative to those of the F_1 ($J = N - 1$) component owing to the large spin-spin constant λ. As a consequence, the rotational spectrum at low rotational temperature approaches that of $^1\Sigma$ molecule when $\lambda \gg B_0$, in which only levels of the F_1 component are thermally populated, and the pattern-forming quantum number is J; Hund's case (a) limit. For both SiC_5 and odd-carbon chains up to C_8S, however, small but significant deviations from harmonicity – beyond those expected from centrifugal distortion alone – are manifest in the spectrum, and allow λ to be determined in a least-squares fit. For GeC_5, how-

Table 1 Measured and *ab initio* rotational constants of GeC_4, GeC_5, and GeC_6 (in MHz).

Species	$B_{0\ \mathrm{exp}}$ [a]	$B_{0\ \mathrm{calc}}$ [b]	Q [d]
$^{70}GeC_4$	1036.4053(2)	1035.718/1036.406[c]	0.07/-6×10^{-5}
$^{72}GeC_4$	1027.0435(2)	1026.365/1027.047[c]	
$^{74}GeC_4$	1018.1423(1)	1017.473/1018.148[c]	
$^{76}GeC_4$	1009.6690(2)	1009.009/1009.678[c]	
$^{70}GeC_5$	617.48402(3)	619.630	-0.3
$^{72}GeC_5$	611.47529(1)	613.596	
$^{74}GeC_5$	605.75309(6)	607.850	
$^{76}GeC_5$	600.29762(2)	602.372	
$^{70}GeC_6$	412.90688(3)	412.926	-0.005
$^{72}GeC_6$	408.70900(1)	408.730	
$^{74}GeC_6$	404.70546(1)	404.727	
$^{76}GeC_6$	400.88084(1)	400.904	

[a] Uncertainties in parentheses are 1σ in the units of the last significant digit. The complete set of spectroscopic constants, derived from the measurements in Tables S1–3, is given in Table S7.†
[b] Calculated from the CCSD(T)/cc-pwCVQZ structure and fc-CCSD(T)/cc-pVDZ zero-point vibrational corrections, see supplementary material, except when otherwise noted.
[c] Calculated from the CCSD(T)/cc-pwCVQZ structure and fc-CCSD(T)/cc-pVTZ zero-point vibrational corrections, see supplementary material.
[d] The percentage difference, calculated as $\frac{B_{0\ \mathrm{exp}} - B_{0\ \mathrm{calc}}}{B_{0\ \mathrm{exp}}}$.

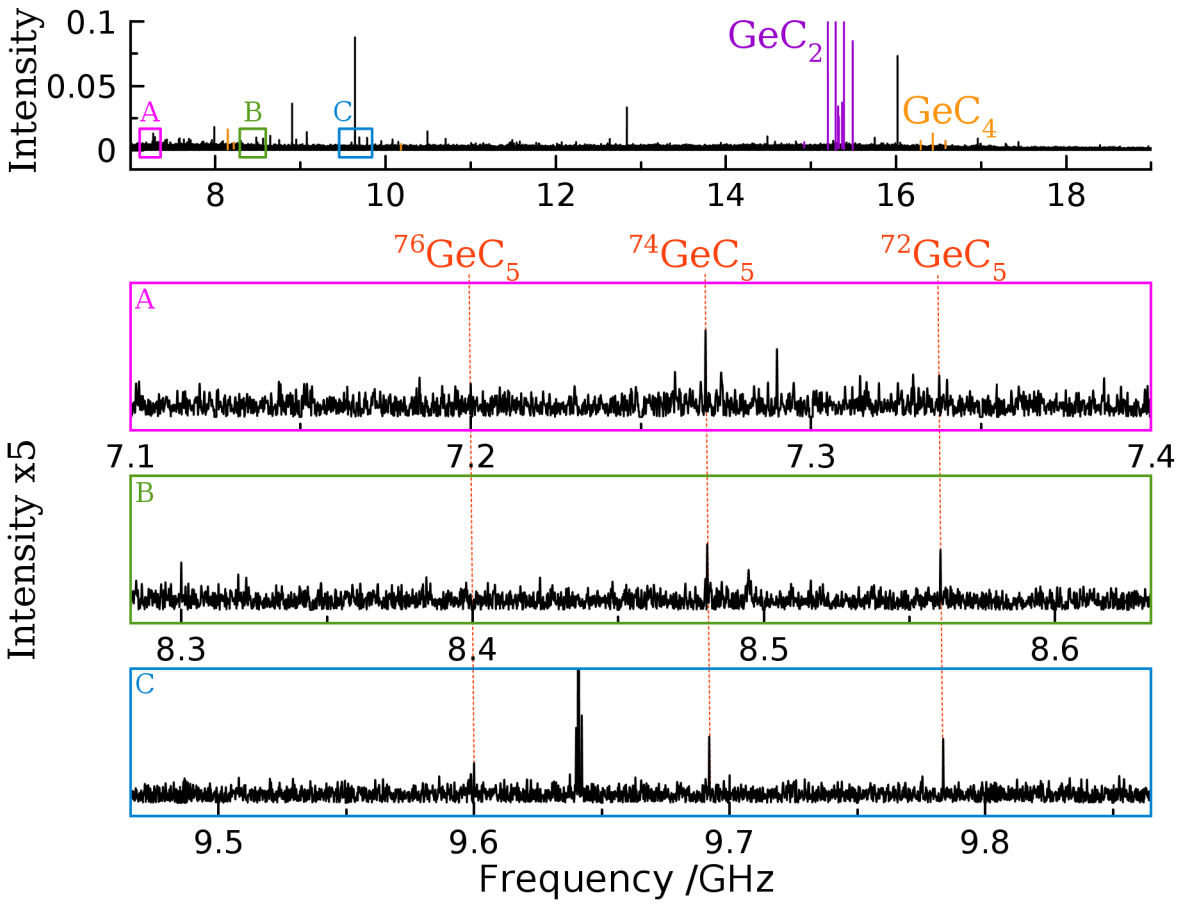

Fig. 2 The broadband rotational spectrum between 7 and 18 GHz in which a Ge:C rod (1:2 by molar ratio) was ablated with the 532 nm frequency-doubled output of a Nd:YAG laser, and the products, entrained in Ne buffer gas, adiabatically expanded into a large vacuum chamber. The top trace displays the entire 11 GHz spectrum with contribution from electronic artifacts and known molecules removed. The $1_{0,1} \rightarrow 0_{0,0}$ transition of $^{74}GeC_2$ and its less abundant Ge isotopic species are conspicuous near 15.3 GHz in the top spectrum and thus the intensity axis has been normalized to the strongest transition of this species (consequently, most transitions of GeC_2 are been truncated in the displayed spectrum). Three series of harmonically-related lines are visible in lower traces (portions of the broadband spectrum in which the vertical scale has been expanded by a factor 5); the strongest features were ultimately assigned to $^{74}GeC_5$ and $^{72}GeC_5$, and the weaker one to $^{76}GeC_5$.

ever, no such deviations are apparent: line frequencies only differ from ratios of integers by that expected from D_0, implying a very large value of λ. The rotational lines of $^{74}GeC_5$, for example, can be reproduced to a fraction of the 2 kHz measurement uncertainty with only two free parameters, B_0=605.75309(6) MHz and $D_0 = 8.3(5) \times 10^{-6}$ MHz. By comparison, closed-shell SiC_6 has very similar rotational and centrifugal distortion constants [B_0=611.25102(6) MHz and $D_0 = 5.5(2) \times 10^{-6}$ MHz] [12]. From simulations using a $^3\Sigma$ Hamiltonian and different values for λ, this parameter must be at least 770 GHz, and, as a consequence, was simply constrained in the final fits. The best-fit rotational constants for GeC_5 using a $^1\Sigma$ Hamiltonian are summarized in Table 1.

4.3 GeC_6

While the longest GeC_n chain considered in this work was not directly observed in the broadband spectrometer, the search for $^{74}GeC_6$ was carried out based on quantum chemical predictions. Confidence based on the GeC_4 experimental and theoretical work, we attempted to exploit the systematic deviation between the electronic structure prediction and the experimental rotational constant: by calculating B_e at the CCSD(T)/cc-pwCVTZ level of theory for both GeC_4 and GeC_6, the search began by scaling the *ab initio* B_e for GeC_6 by the ratio B_0/B_e (1.0018) derived from the GeC_4 results. The basis for this scaling is to account for the vibrational corrections to B_e, with the assumption that the electronic structure is described equally well and indifferent between the two species. Somewhat later in the

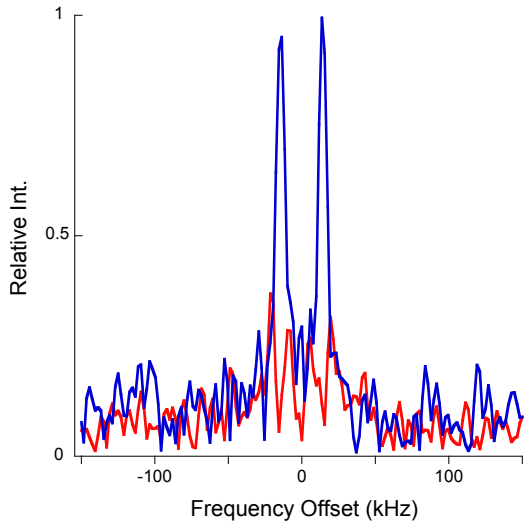

Fig. 3 The $7_6 \rightarrow 6_5$ rotational line of $^{74}GeC_5$ recorded in the absence (blue) and presence (red) of a weak magnetic field. The spectrum is displayed as a frequency offset from the rest frequency of 7269.030 MHz, and its line shape is instrumental in origin; it consists of two well-resolved Doppler components because the supersonic jet expands along the axis of the Fabry-Peŕot cavity. Both spectra are co-averages of approximately 1750 gas pulses, requiring about 6 min of integration at the 5 Hz repetition rate of the nozzle.

study, the CCSD(T)/cc-pwCVQZ equilibrium rotational constant and CCSD(T)/cc-pVDZ vibrational correction also became available. The B_0 rotational constants derived using these two different methods are 403.745 and 404.727 MHz, respectively.

A subsequent search using the cavity spectrometer revealed six lines with relatively high SNR with approximately harmonic separation. By scaling the predicted rotational constants for other isotopologues, additional transitions belonging to $^{70}GeC_6$, $^{72}GeC_6$, and $^{76}GeC_6$ were quickly found. Analogous to the GeC_4 work earlier in this paper, the observed transitions were analyzed and fit to a linear molecule Hamiltonian comprising only of B_0 and D_0 terms. The determined B values of GeC_6 are shown in Table 1. We note here that, while the empirical scaling factor was sufficiently accurate for a deep cavity search, the results highlight the importance of accurate vibrational corrections from first-principles, which provided a calculated B_0 substantially closer to the final experimental value.

4.4 Determination of Ge–C bond lengths

While the experimental data sets collected here do not permit derivations of complete empirical molecular (semi-experimental, r_e^{emp}) structures[58], from the rotational constants of isotopic GeC_4, GeC_5 and GeC_6 it is possible to determine highly accurate Ge–C bond lengths for all three carbides. To do this, the experimental rotational constants were corrected for zero-point vibrational effects at the fc-CCSD(T)/cc-pVTZ (GeC_4) and CCSD(T)/cc-pVDZ (all three chains) levels of theory, the C=C bond lengths were constrained to values derived at the ae-CCSD(T)/cc-pwCVQZ level, and the Ge–C bond length was then least-squares-optimized[59] to reproduce the semi-experimental equilibrium moments of inertia of the isotopic species (see supplementary material). This procedure yields a Ge−C bond length of 1.7757/1.7742 Å for GeC_4 (for the cc-pVTZ/cc-pVDZ zero-point vibrational corrections, respectively), 1.8175 Å for GeC_5, and 1.7820 Å for GeC_6, with 1σ statistical uncertainties well below 10^{-4} Å.

Since the C=C bond lengths were constrained in the optimization and the experimentally derived rotational constants of GeC_5 are model dependent (i.e., on the assumed value of λ), more conservative uncertainties are on the order of a few mÅ for the singlet species (see, e.g., Ref.[60] and references therein) and presumably of order 10 mÅ (1 pm) for GeC_5. Nevertheless, all Ge-C bond lengths derived here from experiment compare very favorably to those predicted at the ae-(U)CCSD(T)/cc-pwCVQZ level of theory, and more generally indicative of a double bond between these two atoms. For comparison, methyl germane, CH_3GeH_3, may serve as a prototypical system featuring a Ge−C single bond. From microwave experiments[61] and at the CCSD(T)/cc-pwCVQZ level of theory (calculated in this work) bond lengths of 1.9453(5) Å and 1.9454 Å, respectively, have been obtained, corresponding to an elongation of more than 0.1 Å compared to the three chains studied here. By way of further comparison, the Ge–C r_e^{emp} semi-experimental bond length is 1.770(1) Å in GeC_3Ge,[14] and 1.77579(21) Å in GeCH[62] suggesting beyond diatomic GeC (1.805 Å)[13] that the Ge–C double bond length in cumulenes is fairly insensitive to the length of the carbon chain and therefore implying that electronic density between Ge−C remains relatively localized from the rest of the conjugated chain. The species with triplet multiplicity (GeC/GeC_5) possess slightly longer heavy atom-carbon bonds (∼1.81 Å) compared to the singlet chains (GeC_4/GeC_6 ∼1.78 Å) – a finding very similar to the situation in isovalent SiC_n species[63,64] – and is consistent with repulsion due to the unpaired electronic configuration.

4.5 Comparison of SiC_n and GeC_n production

Because identical cavity experiments were performed with Si:C and Ge:C rods, a systematic comparison of the production of the two group 14 carbides by laser ablation is possible. Since Si_3[8] and other Si carbides such as Si_2C[7] and rhomboidal SiC_3[10] have been previously studied by cavity spectroscopy and have strong, low-J transitions in the 7–18 GHz frequency range, it is also possible to quantify their production under the same experimental conditions.

For each species, relative intensities were first corrected for the natural abundance of isotopic species, and then converted to relative abundances by factoring the respective rotational par-

tition functions at T_{rot}=5 K and dipole moments. The temperature was chosen to reflect the estimated rotational temperature of our molecular beam, determined by measurements with laser ablation experiments on TiO_2. For the SiC_n species, literature dipole moments were used while for the GeC_n species the dipole moments were calculated at the CCSD(T)/cc-pwCVTZ level; the values used are organized into Table 2. The resulting abundances (relative to XC_2, X = Ge,Si) are shown in Figure 4.

Two important results arise from Figure 4: (I) the abundances of each carbon chain are quite similar between Ge and Si chains, and (II) the linear fits show two different slopes/rates in the abundance. Between one and four units of carbon, the abundance of both Si and Ge species span approximately three orders of magnitude while from four to eight carbon atom chains, the abundance decreases only by an order of magnitude. While the dynamics of formation are not entirely clear, a main contributing factor in their detection would be the dipole moment, which appears to grow steadily with the length of carbon chain (Table 2). Thus, while the production of longer species is expected to diminish, Figure 4 shows that the abundance of long Si and Ge chains, with up to eight atoms for Si−C, is sufficiently high that they remain detectable following a feasible (∼30 minutes) integration time in a cavity experiment, providing accurate predictions of the rotational transitions are available.

Table 2 Dipole moments, in Debye, used to calculate the relative abundances of SiC_n and GeC_n species. With the exception of SiC_2 (which has been experimentally determined), the values tabulated here are calculated using various *ab initio* methods. Dipole moments for the GeC_n chains, which are unique to this work, are calculated at the CCSD(T)/cc-pwCVTZ level.

n^a	SiC_n	Ref.	GeC_n	Ref.
1	0.9		-	
2	2.4	65	3.1	19
3	4.8, 2.1, 4.2[b]	66–68	-	
4	6.4	63	7.0	this work
5	6.6	66	6.6	this work
6	8.3	63	8.8	this work
7	7.3		-	
8	10.0		-	

[a]Number of carbon atoms
[b]Corresponds to the linear, cyclic oblate, and cyclic prolate forms of SiC_3, respectively.

5 Discussion

Based on a combination of CP and cavity FTMW spectroscopies, we were able to characterize three new Ge−C chains, two of which were readily abundant and detectable by CP FTMW spectroscopy (GeC_4 and GeC_5), and the remaining GeC_6 was subsequently found in the cavity. As a general comment, it appears that the electronic structure of Ge−C chains are similar to Si−C and other carbon-chains, displaying the same odd-even triplet/singlet electronic ground state alternation, although as we shall discuss in the following passages, there are a few subtleties regarding the electronic structure of Ge−C species that require further elaboration.

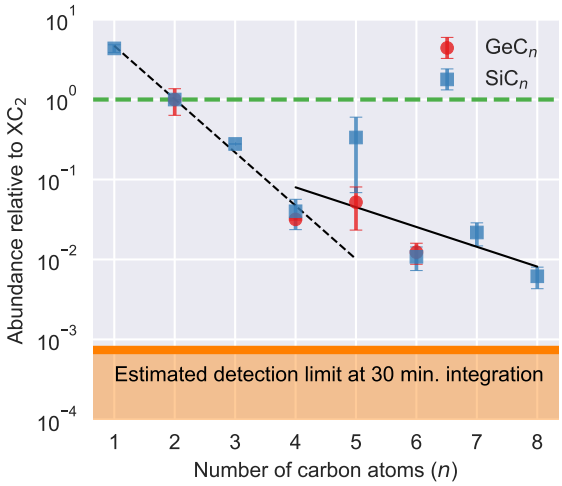

Fig. 4 The abundance of SiC_n (blue squares) and GeC_n (red circles) species, relative to their respective dicarbides as observed in the microwave cavity experiments. Error bars represent 2σ uncertainties. The SiC_3 point is given as the cumulative abundance of the linear and rhombic forms. The estimated detection limit is based on the noise floor of a 1 MHz window following 30 min of integration in the cavity instrument.

It is somewhat surprising that the ground state of GeC_5 radical is so close to the Hund's case (a) limit that its spin-spin coupling constant can not be determined even from high-resolution rotational data with sub-ppm fractional accuracy. As a point of comparison, this constant is 31.5 GHz for SiC_5, while a lower limit of ∼770 GHz is derived here. This constant includes second-order spin-orbit interactions between the triplet ground state and a low-lying singlet electronic state,[69] so such a large value likely indicates that the unpaired electrons have significant density at the heteroatom, owing to the ∼10 fold increase in the spin-orbit constant of Ge or Ge^+ (904 and 1178 cm^{-1}, respectively)[70] relative to either Si or Si^+ (149 and 191 cm^{-1}, respectively). Although the energy gap between the two states may also be smaller in GeC_5, no theoretical calculations or experimental data on electronically excited states are available for Ge carbides beyond GeC.

The present work suggests that despite the heavier mass of Ge and increased importance of relativistic factors for third-row elements, CCSD(T)/cc-pwCVXZ (X =T, Q) can still be used with considerable confidence to predict the structures of other small Ge-bearing species – that is to say that the electronic structure is adequately described by coupled-cluster theory with modestly-sized

basis sets. For the three Ge−C_n chains reported here, the theoretical rotational constants reproduce the experimentally determined values to within ∼0.2%. Further evidence that this agreement is not fortuitous is provided by the close agreement between the calculated and best-fit Ge−C bond lengths.

Where the rotational constants have been used to bridge the theory and experiment, additional comparisons could be made on the dipole moment of these species; as a property related to the electronic density, and therefore the quality of the electronic wavefunction, measurement of the dipole moment would allow a direct comparison between theory and experiment. In this light, an experimental determination of the electric dipole of GeC_n may prove illuminating – in addition to the usual, well-known difficulties in retrieving electron correlation in metal carbide chains[63], the inclusion of a third-row element provides an opportunity to benchmark relativistic contributions to molecular electronic wavefunctions. Owing to the low fractional ionization of laser ablation, the dipole moment of SiC_2, produced in a similar fashion than in the present work, was measured long ago using FT cavity spectroscopy and a Stark cage.[65] Such a measurement for GeC_2 would appear to be possible: its fundamental line is very intense and a Stark cage[71] was made available for use in our CP chamber. Since GeC_4 and GeC_5 were observable in the CP spectrum, conceivably the dipole moments of GeC_2, GeC_4, and GeC_5 could be measured simultaneously in one experiment.

In addition to testing *ab initio* theories, the experimental work here furthers the detection of long chain metal carbide species. As seen in Figure 4, the production of Si- and Ge-carbides is remarkably similar in our experiments: both dicarbides are produced in very high abundance, while the longer four-, five-, and six-carbon carbides, while readily detectible, are roughly present at a few percent of this level. The absence of rotational lines of linear SiC_3, however, and the apparent absence of lines that can be attributed to analogous GeC_3 species is slightly puzzling. Previous studies of the SiC_3 isomers suggested that kinetic factors favored formation of the linear chain compared to the ring-like isomers at short gas durations and lower pressure pressures, presumably owing to entropic factors. At more typical expansion conditions, however, the thermodynamically more stable product, the oblate isomer of rhombic SiC_3. Drawing a parallel between the earlier SiC_n work and the new frontiers of GeC_n, the apparent absence of GeC_3, along with GeC_7 and GeC_8 appears technical rather than fundamental; both species should be present, albeit at somewhat lower abundance compared to their longer carbides counterparts. Subsequent searches can be carried out, providing *ab initio* predictions of their structures are sufficiently accurate to constrain the search range to feasible integration time. Additionally, based on the observed decrease in abundance decrement, the detection of progressively longer chains XC_n, where X =Ge,Si and $n > 8$, would similarly be achievable. Efforts in this direction will likely contribute to the understanding of how metal-bearing carbon chains grow, from a thermodynamic and kinetic perspective.

Laser ablation has been used successfully to generate and detect diatomic and relatively small polyatomic species in the radio band; there are by comparison relatively few examples were larger metal-bearing species have been detected by similar means. It is well known from mass spectrometric investigations, however, that much larger clusters are readily formed under similar conditions. Presumably the limitation in detecting their pure rotational transitions is a combination of less efficient production with increasing molecule size and the sensitivity of the method. As the present work demonstrates, with improvements in one or both areas, modestly larger clusters can now be detected, suggesting that the same basic approach might be used with good success to characterize other large metal-bearing species.

6 Conclusions

Combining CP- and cavity FTMW spectroscopy with laser ablation, we present the discovery and spectroscopic characterization of three new germanium-bearing carbon chain species. Upon discovery of GeC_2 in the CP spectrum[19], evidence for the GeC_4 and GeC_5 chains were found soon afterwards in the same spectrum based on high-level quantum-chemical calculations. An additional third species, GeC_6, was discovered with cavity measurements, once again relying on high-level calculations. Drawing parallels to the closely related SiC_n chains, the spectroscopy of the three species was reproduced readily with simple linear $^1\Sigma$ Hamiltonians, including the curious case of GeC_5, which should require a $^3\Sigma$ model. Despite the fact that the value of λ for this species is thought to be large, the experimental frequencies are well-reproduced using an effective $^1\Sigma$ Hamiltonian, which may motivate first principles determination of this parameter. Finally, the relative abundances of Ge−C and Si−C chains in the ablation experiment were compared using cavity FTMW measurements. The results show a remarkable similarity between the two metal bearing carbon chains, suggesting that the analogous GeC_3, GeC_7, and GeC_8 species should, in theory, be present and detectable. The decrement in abundance towards longer XC_n (where X = Ge, Si and $n > 4$) carbon chains appears to be fairly flat, contrary to the rapid decrease in relative abundance of the shorter ($n < 4$) chains. The fortuitous sustained detectability will hopefully inspire not only subsequent searches for the remaining GeC_n species, but also longer chains of SiC_n as well as other metal-bearing carbon-rich molecules.

Acknowledgments

We thank Michael E. Harding for helpful discussions, and Oliver Zingsheim for help in the original CP experiments. M. C. M. and K. L. K. L. acknowledge NSF grant AST-1615847 for financial support. Research of carbon clusters in Cologne is carried

out within the Collaborative Research Centre 956, sub-project B3, funded by the Deutsche Forschungsgemeinschaft (DFG) - project ID 184018867. S. T. is grateful to the DFG for additional support through grants TH 1301/3-2 and SCHL 341/15-1 (*Cologne Center for Terahertz Spectroscopy*). We also thank the Regional Computing Center of the Universität zu Köln (RRZK) for providing computing time on the DFG-funded High Performance Computing (HPC) system CHEOPS. M.-A. M.-D. is thankful to the Programme National "Physique et Chimie du Milieu Interstellaire" (PCMI) of CNRS/INSU with INC/INP co-funded by CEA and CNES for support.

References

1 A. Van Orden and R. J. Saykally, *Chem. Rev.*, 1998, **98**, 2313–2357.
2 S. L. Wang, C. M. L. Rittby and W. R. M. Graham, *J. Chem. Phys.*, 1997, **107**, 6032–6037.
3 S. L. Wang, C. M. L. Rittby and W. R. M. Graham, *J. Chem. Phys.*, 1997, **107**, 7025–7033.
4 R. Nagarajan and J. P. Maier, *Int. Rev. Phys. Chem.*, 2010, **29**, 521–554.
5 M. C. McCarthy, C. A. Gottlieb and P. Thaddeus, *Mol. Phys.*, 2003, **101**, 697–704.
6 D. Michalopoulos, M. Geusic, P. Langridge-Smith and R. Smalley, *J. Chem. Phys.*, 1984, **80**, 3556–3560.
7 M. C. McCarthy, J. H. Baraban, P. B. Changala, J. F. Stanton, M. A. Martin-Drumel, S. Thorwirth, C. A. Gottlieb and N. J. Reilly, *J. Phys. Chem. Lett.*, 2015, **6**, 2107–2111.
8 M. C. McCarthy and P. Thaddeus, *Phys. Rev. Lett.*, 2003, **90**, 213003.
9 M. C. McCarthy, A. J. Apponi and P. Thaddeus, *J. Chem. Phys.*, 1999, **110**, 10645–10648.
10 A. J. Apponi, M. C. McCarthy, C. A. Gottlieb and P. Thaddeus, *J. Chem. Phys.*, 1999, **111**, 3911–3918.
11 M. C. McCarthy, A. J. Apponi and P. Thaddeus, *J. Chem. Phys.*, 1999, **111**, 7175–7178.
12 M. McCarthy, A. Apponi, C. Gottlieb and P. Thaddeus, *Astrophys. J.*, 2000, **538**, 766–772.
13 C. R. Brazier and J. I. Ruiz, *J. Mol. Spectrosc.*, 2011, **270**, 26 – 32.
14 S. Thorwirth, V. Lutter, A. Javadi Javed, J. Gauss and T. F. Giesen, *J. Phys. Chem. A*, 2016, **120**, 254–259.
15 D. L. Robbins, C. M. L. Rittby and W. R. M. Graham, *J. Chem. Phys.*, 2001, **114**, 3570–3574.
16 E. Gonzalez, C. M. L. Rittby and W. R. M. Graham, *J. Chem. Phys.*, 2006, **125**, 044504.
17 E. Gonzalez, C. M. L. Rittby and W. R. M. Graham, *J. Chem. Phys.*, 2009, **130**, 194511.
18 D. L. Robbins, K.-C. Chen, C. M. L. Rittby and W. R. M. Graham, *J. Chem. Phys.*, 2004, **120**, 4664–4671.
19 O. Zingsheim, M.-A. Martin-Drumel, S. Thorwirth, S. Schlemmer, C. A. Gottlieb, J. Gauss and M. C. McCarthy, *J. Phys. Chem. Lett.*, 2017, **8**, 3776–3781.
20 L. Sari, K. A. Peterson, Y. Yamaguchi and H. F. Schaefer, *J. Chem. Phys.*, 2002, **117**, 10008–10018.
21 P. Wielgus, S. Roszak, D. Majumdar and J. Leszczynski, *J. Chem. Phys.*, 2005, **123**, 234309.
22 V. M. Rayón, P. Redondo, C. Barrientos and A. Largo, *J. Chem. Phys.*, 2010, **133**, 124306.
23 S. Goswami, S. Saha and R. Yadav, *Physica E*, 2015, **74**, 175 – 192.
24 S. K. Parida, S. Sahu and S. Sharma, *Chem. Phys. Lett.*, 2016, **659**, 216 – 220.
25 B. Kleman, *Astrophys. J.*, 1956, **123**, 162–165.
26 A. K. Ray and M. N. Huda, *J. Comput. Theor. Nanosci.*, 2006, **3**, 315–341.
27 P. Mélinon, B. Masenelli, F. Tournus and A. Perez, *Nat. Mater.*, 2007, **6**, 479–490.
28 K. H. Seng, M.-H. Park, Z. P. Guo, H. K. Liu and J. Cho, *Angew. Chem. Int. Ed.*, 2012, **51**, 5657–5661.
29 P. Venezuela, G. M. Dalpian, A. J. R. da Silva and A. Fazzio, *Phys. Rev. B*, 2001, **64**, 193202.
30 A. Benzair, B. Bouhafs, B. Khelifa, C. Mathieu and H. Aourag, *Phys. Lett. A*, 2001, **282**, 299 – 308.
31 C. Jo and K. Lee, *J. Chem. Phys.*, 2000, **113**, 7268–7272.
32 S.-D. Li, Z.-G. Zhao, X.-F. Zhao, H.-S. Wu and Z.-H. Jin, *Phys. Rev. B*, 2001, **64**, 195312.
33 C. R. Brazier, L. C. O'Brien and P. F. Bernath, *J. Chem. Phys.*, 1989, **91**, 7384–7386.
34 R. W. Schmude, K. A. Gingerich and J. E. Kingcade, *J. Phys. Chem.*, 1995, **99**, 15294–15297.
35 G. G. Brown, B. C. Dian, K. O. Douglass, S. M. Geyer, S. T. Shipman and B. H. Pate, *Rev. Sci. Instrum.*, 2008, **79**, 053103.
36 T. J. Balle and W. H. Flygare, *Rev. Sci. Instrum.*, 1981, **52**, 33–45.
37 K. N. Crabtree, M.-A. Martin-Drumel, G. G. Brown, S. A. Gaster, T. M. Hall and M. C. McCarthy, *J. Chem. Phys.*, 2016, **144**, 124201.
38 M. C. McCarthy, L. Zou and M.-A. Martin-Drumel, *J. Chem. Phys.*, 2017, **146**, 154301.
39 B. A. McGuire, M.-A. Martin-Drumel, K. L. K. Lee, J. F. Stanton, C. A. Gottlieb and M. C. McCarthy, *Phys. Chem. Chem. Phys.*, 2018, **20**, 13870–13889.
40 S. Brünken, H. S. P. Müller, K. M. Menten, M. C. McCarthy and P. Thaddeus, *Astrophys. J.*, 2008, **676**, 1367–1371.
41 M. C. McCarthy, M. J. Travers, A. Kovacs, C. A. Gottlieb and P. Thaddeus, *Astrophys. J. Suppl. Ser.*, 1997, **113**, 105–120.

42 M. C. McCarthy, W. Chen, M. J. Travers and P. Thaddeus, *Astrophys. J. Suppl. Ser.*, 2000, **129**, 611–623.

43 C. A. Gottlieb, A. J. Apponi, M. C. McCarthy, P. Thaddeus and H. Linnartz, *J. Chem. Phys.*, 2000, **113**, 1910–1915.

44 K. Raghavachari, G. W. Trucks, J. A. Pople and M. Head-Gordon, *Chem. Phys. Lett.*, 1989, **157**, 479–483.

45 CFOUR, a quantum chemical program package written by J. F. Stanton, J. Gauss, M. E. Harding, P. G. Szalay with contributions from A. A. Auer, R. J. Bartlett, U. Benedikt, C. Berger, D. E. Bernholdt, Y. J. Bomble, L. Cheng, O. Christiansen, M. Heckert, O. Heun, C. Huber, T.-C. Jagau, D. Jonsson, J. Jusélius, K. Klein, W. J. Lauderdale, D. A. Matthews, T. Metzroth, L. A. Mück, D. P. O'Neill, D. R. Price, E. Prochnow, C. Puzzarini, K. Ruud, F. Schiffmann, W. Schwalbach, S. Stopkowicz, A. Tajti, J. Vázquez, F. Wang, J. D. Watts and the integral packages MOLECULE (J. Almlöf and P. R. Taylor), PROPS (P. R. Taylor), ABACUS (T. Helgaker, H. J. Aa. Jensen, P. Jørgensen, and J. Olsen), and ECP routines by A. V. Mitin and C. van Wüllen. For the current version, see http://www.cfour.de.

46 M. E. Harding, T. Metzroth, J. Gauss and A. A. Auer, *J. Chem. Theory Comput.*, 2008, **4**, 64–74.

47 T. H. Dunning, *J. Chem. Phys.*, 1989, **90**, 1007–1023.

48 T. Van Mourik and T. H. Dunning, *Int. J. Quantum Chem.*, 2000, **76**, 205–221.

49 D. E. Woon and T. H. Dunning, *J. Chem. Phys.*, 1995, **103**, 4572–4585.

50 K. A. Peterson and T. H. Dunning, *J. Chem. Phys.*, 2002, **117**, 10548–10560.

51 N. B. Balabanov and K. A. Peterson, *J. Chem. Phys.*, 2005, **123**, 064107.

52 N. J. DeYonker, K. A. Peterson and A. K. Wilson, *J. Phys. Chem. A*, 2007, **111**, 11383–11393.

53 J. Gauss and J. F. Stanton, *Chem. Phys. Lett.*, 1997, **276**, 70–77.

54 W. Schneider and W. Thiel, *Chem. Phys. Lett.*, 1989, **157**, 367–373.

55 J. F. Stanton, C. L. Lopreore and J. Gauss, *J. Chem. Phys.*, 1998, **108**, 7190–7196.

56 J. N. Oliveira, M.-A. Matrin-Drumel and M. C. McCarthy, *SPECDATA: Automated Analysis Software for Broadband Spectra*, 10.5281/zenodo.400323, 2017.

57 V. D. Gordon, M. C. McCarthy, A. J. Apponi and P. Thaddeus, *Astrophys. J. Suppl. Ser.*, 2001, **134**, 311–317.

58 J. Vázquez and J. F. Stanton, in *Equilibrium Molecular Structures - From Spectroscopy to Quantum Chemistry*, ed. J. Demaison, J. E. Boggs and A. G. Csàszár, CRC Press, 2011, pp. 53–87.

59 Z. Kisiel, *J. Mol. Spectrosc.*, 2003, **218**, 58 – 67.

60 C. Puzzarini, *Phys. Chem. Chem. Phys.*, 2013, **15**, 6595–6607.

61 V. W. Laurie, *J. Chem. Phys.*, 1959, **30**, 1210–1214.

62 T. C. Smith, H. Li, D. J. Clouthier, C. T. Kingston and A. J. Merer, *The Journal of Chemical Physics*, 2000, **112**, 8417–8425.

63 V. D. Gordon, E. Nathan, A. Apponi, M. McCarthy, P. Thaddeus and P. Botschwina, *J. Chem. Phys.*, 2000, **113**, 5311–5320.

64 P. Botschwina and R. Oswald, *Z. Phys. Chem.*, 2001, **215**, 393–400.

65 R. D. Suenram, F. J. Lovas and K. Matsumura, *Astrophys. J. Lett.*, 1989, **342**, L103–L105.

66 M. C. McCarthy, A. J. Apponi, C. A. Gottlieb and P. Thaddeus, *Astrophys. J.*, 2000, **538**, 766.

67 H. S. P. Müller and D. E. Woon, *J. Phys. Chem. A*, 2013, **117**, 13868–13877.

68 I. Alberts, R. Grev and H. Schaefer III, *J. Chem. Phys.*, 1990, **93**, 5046–5052.

69 W. Gordy and R. L. Cook, *Microwave Molecular Spectra*, Wiley, 1970.

70 H. Lefebvre-Brion and R. W. Field, *Perturbations in the Spectra of Diatomic Molecules*, Academic Press, 1986.

71 T. Emilsson, H. S. Gutowsky, G. de Oliveira and C. E. Dykstra, *J. Chem. Phys.*, 2000, **112**, 1287–1294.